WATER ICE CLOUDS AND THERMAL STRUCTURE IN THE MARTIAN TROPICS AS REVEALED BY MARS CLIMATE SOUNDER.

R. J. Wilson , *NOAA/Geophysical Fluid Dynamics Laboratory, Princeton, NJ, USA (John.Wilson@noaa.gov).*

Introduction: The MGS mission returned suggestive evidence for the influence of radiatively active water ice clouds on tropical temperature structure during the NH summer solstice season when an equatorial cloud belt is observed to be prominent. Elevated tropical temperature inversions were strikingly evident in early morning (~0400 LT) tropical temperature profiles derived from MGS Radio Science (RS) occultations during the L_s=140-156° period in MY24 [*Hinson and Wilson*, 2004]. With the aid of a Mars GCM, these inversions were interpreted as the manifestation of a topographically modulated thermal tide that is amplified by the radiative forcing associated with the embedded water ice clouds. The sparse coverage of RS observations and the coarse vertical resolution of the TES nadir and limb retrievals constrained the development of a comprehensive description of the temporal and spatial structure of the coupled tropical cloud and thermal fields. The recent refinement of the version 3 temperature retrievals (based on limb and off-nadir profiling) from Mars Climate Sounder (MCS) provides sufficient vertical resolution to clearly identify the temperature inversions previously seen only in the MGS RS profiles [*Shirley et al*., 2010]. The ability to retrieve profiles of water ice cloud opacity allows for exploring the relationship between clouds and temperature. We will make use of a MGCM to contrast the simulated tide responses to forcing by clouds and topography with the available observations.

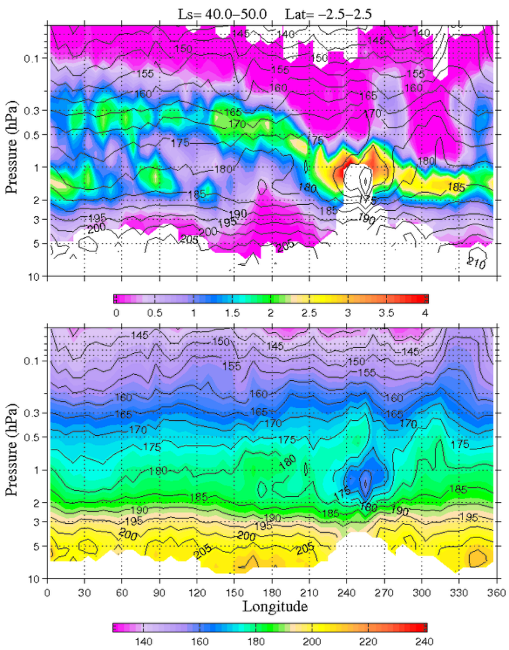

Figure 1. (a) Longitude-pressure distribution of water ice cloud opacity (color) and temperature (contours) derived from 0300 LT MCS retrievals in MY29 (L_s=40-50°). Opacity units are 10^{-3}/km and temperature is contoured at intervals of 5 K. (b) Temperature redisplayed in color.

MCS Results: MCS is an infrared radiometer in a polar, sun-synchronous orbit (0300 &1500 LT) using limb and on-planet viewing. The limb profiles allow temperature and aerosol retrievals from 5-10 km to ~80 km in height, with a vertical resolution of ~5 km [*Kleinbohl et al*. 2009]. MCS has roughly the same nominal resolution as TES limb observations, but in practice we are finding that MCS is able to resolve more vertical detail than TES. A limitation of MCS is that low level clouds can restrict the vertical extent of retrievals. These are expected to be particularly prominent in morning temperature tropical profiles and along the polar caps. These new data provide extensive latitude and longitude coverage over 2 Mars years.

Figures 1 and 2 show the distribution of equatorial (2.5°S-2.5°N) water ice cloud opacity and temperature as a function of longitude and pressure for the periods of *Ls*= 40-50° and 112-120°, respectively. A striking feature in each case is the cold low-level temperature anomaly in the Tharsis region and an associated temperature maximum aloft. The pattern is quite robust and is present throughout the L_s=20-140° period. Unusually early regional dust

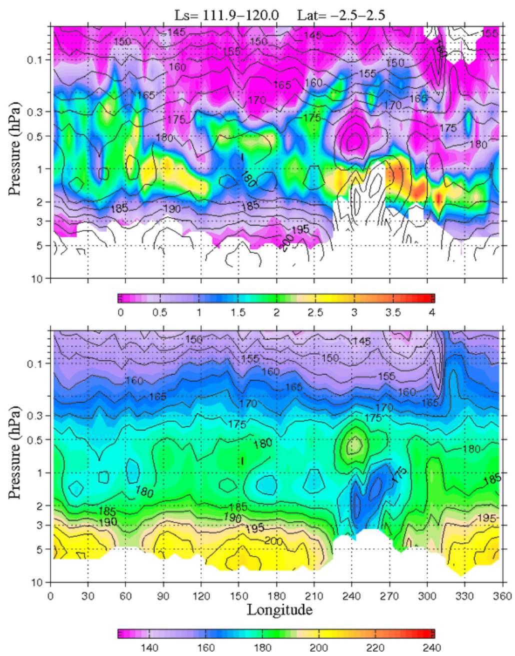

Figure 2. As in Figure 1, but for L_s=112-120° in MY30.

activity around L_s=140° in MY29 disrupted this pattern, which was present past L_s=155° in MY30. The strong temperature inversion in Figure 2 is very similar to that described in *Hinson and Wilson* [2004]. The MCS data strongly suggests that the cold temperature anomaly is coincident with a region of high cloud opacity. It is natural to speculate that the cold anomaly is a consequence of strong radiative cooling by water ice clouds. Note that MCS retrievals are restricted by regions of excessive opacity and so the presence of optically thick low level clouds over Tharsis will need to be inferred by other means. Figure 2 also indicates the presence of relatively cool temperatures in the vicinity of Arabia (70°E). This anomaly develops after L_s =60°, peaks around L_s=110° and subsequently decays.

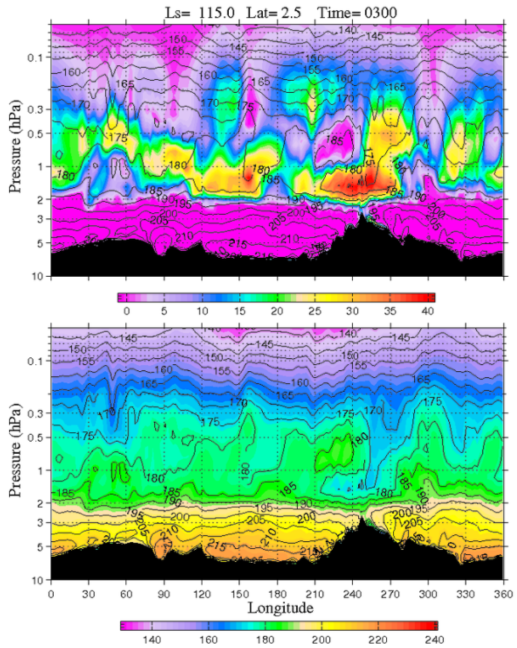

Figure 3. (a) Longitude-pressure distribution of water ice cloud mixing ratio (shading) and temperature (contours) from a MGCM simulation with radiatively active water ice clouds (L_s=115°). Cloud units are ppm. (b) As for a, but temperature is also shaded.

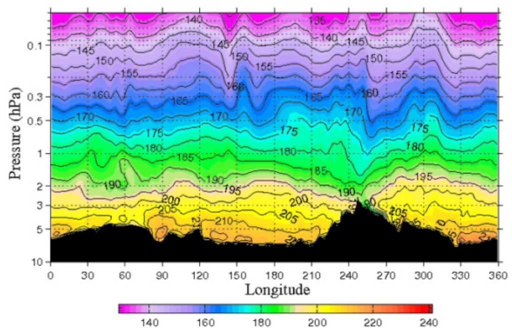

Figure 4. Longitude-pressure distribution of temperature from a MGCM simulation with passive water ice clouds (L_s=115°).

Mars GCM Results: We can study the coupled interaction between water ice clouds and temperature using the GFDL MGCM. The model is described in *Wilson* [2011], but for the purposes of this investigation we note that the radiative effects of water ice clouds are included. In the cloud simulation shown here, a relatively large, uniform cloud radius of 4μm was assumed. Figure 3 shows the simulated cloud and temperature fields for comparison with the MCS observations in figure 2. The simulated temperatures are in general accord with the observations and include a temperature inversion at around 240°E. Note that the observed cloud field is represented by opacity (km^{-1}) while the simulated cloud field is given as a mass mixing ratio. Conversion from opacity to mixing ratio requires knowledge of the effective cloud radius and scattering cross-section. By any reasonable assumption, the simulated cloud mixing ratios appears to be significantly larger than observed, as has been noted by *Heavens et al.* [2010]. The influence of the simulated clouds can be seen by comparing the temperature fields in Figures 3 and 4. Clouds contribute to a net warming of the tropical atmosphere above 1 hPa by absorbing upwelling IR radiation from the relatively hot surface. Of course, this effect is dominant during the day when surface temperatures are hottest. This cloud effect is discussed in *Wilson et al.* [2008] and *Wilson* [2011]. More notably, the clouds lead to increased zonal structure in temperature, with the cold temperature anomaly below 1 hPa due to enhanced nighttime IR emission.

Latitude Comparison: We continue the comparison of model and observations by presenting the latitude structure of clouds and temperature along a longitude running through the Tharsis plateau. These cross-sections are shown in Figures 5 and 6, and follow the same format as Figures 2 and 3. Both data and simulation show an isolated equatorial temperature maximum sitting atop a low-lying cloud layer. The simulated near-surface temperatues are considerably warmer than those in the MCS retrievals. We speculate that this may be due to the absense of cloud between 2 hPa and the surface. Unfortunately, the MCS cloud retrievals are not able to resolve this issue. The MGCM simulation is also anomalously warm in two regions, roughly centered at (35°N, 1 hPa) and (50°S, 0.2 hPa), where the simulation is notably lacking clouds. However, further investigation will be required to assess how the effects of thermal forcing and dynamical response influence the mutual adjustment of the cloud and temperature fields. *Hinson and Wilson* [2004] and *Lee et al.* [2009] argue that the thermal tides strongly shape the cloud response.

Column Cloud Opacity: Figure 7 shows the spatial distribution of MGS MOLA nighttime extinction for the L_s=90-120° season. Regions with high extinction (greater than 0.9) have been associated with optically thick (τ ≥ 1) water ice clouds [*Wilson* *et al.*, 2007]. Evidently there are thick clouds near Syrtis Major and in the Tharsis region, notably more opaque than suggested by extrapolation of the MCS profiles. We speculate that the development of the low-level cold temperature anomaly at 60°E in Figure 2 is related to the clouds in this region.

Figure 8 shows the evolution of surface temperature at a location east of Pavonis Mons. It was argued in *Wilson et al.* [2007] that the rise and fall of the difference between the observed and simulated reference surface temperature is evidence for a significant evolving downward IR flux from water ice clouds. Cloud opacities of ~1 appear to yield sufficient additional IR flux at the surface to account for the observed surface temperature increase at solstice. We are currently working to fit the observed surface brightness temperatures by comparing with simulated brightness temperatures from an ensemble of MGCM runs with varying cloud descriptions. It is noteworthy that the development of the near-surface (below 2 hPa) cold temperature anomaly illustrated in Figures 2 and 3 closely follows the cloud opacity implied by Figure 8.

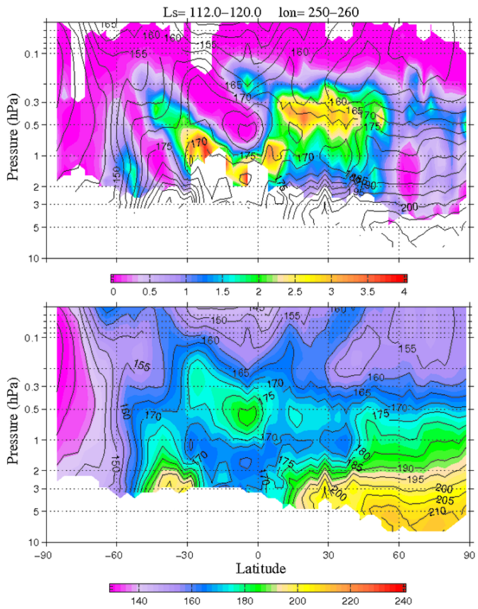

Figure 5. (a) Latitude-pressure distribution of water ice cloud opacity and temperature derived from MCS retrievals. Plotting conventions are the same as in figure 1.

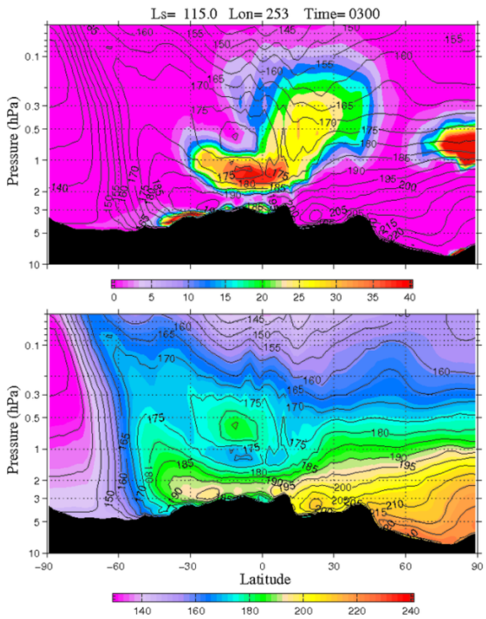

Figure 6. (a) Latitude-pressure distribution of water ice cloud opacity and temperature derived from MGCM simulation with water ice clouds. Plotting conventions are the same as in figure 3.

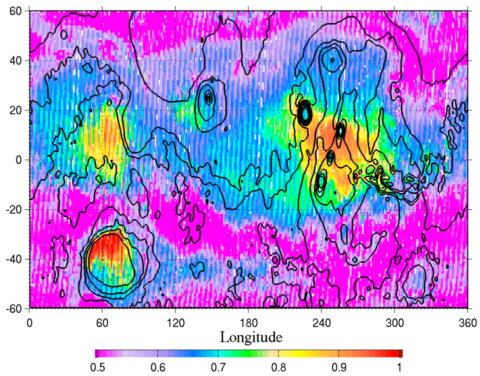

Figure 7. Spatial distribution of atmospheric extinction from MGS MOLA for L_s=90-120°. Regions with high extinction (> 0.9) are associated with optically thick (τ~1) water ice clouds.

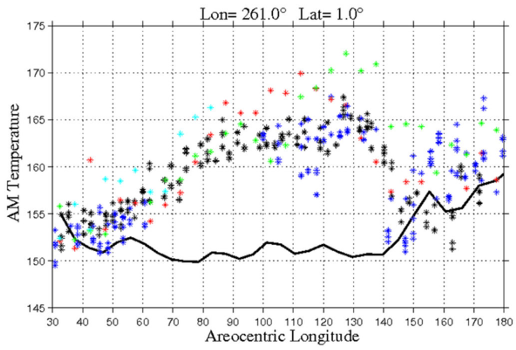

Figure 8. The seasonal evolution of morning (0300 LT) temperatures at a location (4°×4°) in the Tharsis region. MCS surface (32 μm) temperatures are shown in blue and black for MY29 and MY30, respectively and TES (0200 LT) surface temperatures are shown in cyan, red, and green. The black curve is the 32 μm brightness temperature from a MGCM simulation employing an evolving dust column opacity corresponding to TES observations and radiatively passive water ice clouds.

Discussion and Conclusions: The evidence for coupling between tropical clouds and the thermal tide first seen in MGS Radio Science observations has been reinforced with the much more extensive and comprehensive data returned from MCS. The presence of strong elevated nighttime temperature inversions in the Tharsis region is evidently a robust feature of the equatorial atmosphere during the L_s=20-140° season, with little difference seen between the two Mars years examined (MY 29 and 30). The tropical structure appears to evolve over the spring and summer seasons in response to the waxing and waning of tropical cloud opacity. MGCM simulations suggest that radiative forcing by water ice clouds plays a significant role in establishing the observed structure. It is also clear that the modeling results presented here are very crude and that there is considerable need for a more sophisticated treatment of cloud microphysics. Based on our modeling to date, it is expected that a range of ice particle sizes will need to be represented, with smaller particles to match the broad vertical extent of the tropical cloud band and larger particles to account for the more localized and, evidently, strong near-surface cooling in the Tharsis and Arabia regions. We expect that the MCS data will provide valuable guidance and constraints for future model development.

The zonal temperature anomalies in Figures 1 and 2 are related to the tide temperature structure described in *Wilson* [2000] and *Wilson et al*. [2003]. These tides include eastward propagating, diurnal period Kelvin waves and shorter vertical wavelength westward propagating tide modes. The MCS data is confirming the expected presence of these tide modes in the upper atmosphere. The relative lack of interannual variability in the aphelion season suggests that the 4 Mars years of Viking surface pressure can be used as an additional constraint. *Wilson et al*. [2008b] suggested that the diurnal Kelvin wave is prominent in the observed tide record and appears to be sensitive to cloud forcing.

The opportunity that MCS permits of simultaneously retrieving temperature and aerosol profiles with much improved vertical resolution is a major advance in characterizing the Mars atmosphere. We anticipate further discussion and collaboration with the MCS team to better understand the strengths and limitations of the retrieval process. Improved estimation of column aerosol optical depth is one area of focus.

Acknowledgments: This work was supported by grants from the NASA Planetary Atmospheres and Mars Data Analysis programs. Many thanks go to the members of the MCS team, in particular to Tim Schofield and Jim Shirley.

References:

Heavens, N.G., et al. (2010), Water ice clouds over the Martian tropics during northern summer, *Geophys. Res. Lett*., in press.

Hinson, D., and R.J. Wilson (2004), Temperature inversions, thermal tides, and water ice clouds in the martian tropics, *J. Geophys. Res.*, *109*, E01002, doi:10.1029/JE002129.

Kleinböhl, A., et al. (2009), Mars Climate Sounder limb profile retrieval of atmospheric temperature, pressure, and dust and water ice opacity, *J. Geophys. Res., 114*, E10006, doi:10.1029/2009JE003358.

Lee, C., et al., (2009), Thermal tides in the martian middle atmosphere as seen by the Mars Climate Sounder, *J. Geophys. Res., 114*, E03005, doi:10.10129/2008JE003285.

Shirley, J., et al. (2011), Comparison of MGS radio science mean temperature profiles with Mars Climate Sounder (MCS) results, 4th International Workshop on the Mars Atmosphere: Modeling and Observations, Paris.

Wilson, R.J. (2000), Evidence for diurnal period Kelvin waves in the martian atmosphere from Mars Global Surveyor TES data, *Geophys. Res. Lett., 27*, 3889-3892.

Wilson, R.J., D. Banfield, D.P. Hinson, and M.D. Smith (2003), GCM simulation of thermal tides in the Mars atmosphere, Mars atmosphere modeling and observations workshop, Granada, Spain.

Wilson, R.J., G. Neumann, and M.D. Smith (2007), The diurnal variation and radiative influence of martian water ice clouds, *Geophys. Res. Lett*., *34*, L02710, doi:10.1029/2006GL027976.

Wilson, R.J., S.R. Lewis, and L. Montabone (2008), Influence of water ice clouds on Martian tropical atmospheric temperatures, *Geophys. Res. Lett., 35*, L07202, doi:10.1029/2007GL032405.

Wilson, R.J., S.R. Lewis, and L. Montabone (2008b), Thermal tides in an assimilation of three years of TES data from Mars Global Surveyor, Abstract 9022, Mars Atmosphere: Modeling and Observations Workshop, Williamsburg, VA.

Wilson, R.J., (2011), Dust cycle modeling with the GFDL Mars general circulation model, 4th International Workshop on the Mars Atmosphere: Modeling and Observations, Paris.